CHAPTER

2 The wireless channel

A good understanding of the wireless channel, its key physical parameters and the modeling issues, lays the foundation for the rest of the book. This is the goal of this chapter.

A defining characteristic of the mobile wireless channel is the variations of the channel strength over time and over frequency. The variations can be roughly divided into two types (Figure 2.1):

- *Large-scale fading*, due to path loss of signal as a function of distance and shadowing by large objects such as buildings and hills. This occurs as the mobile moves through a distance of the order of the cell size, and is typically frequency independent.
- *Small-scale fading*, due to the constructive and destructive interference of the multiple signal paths between the transmitter and receiver. This occurs at the spatial scale of the order of the carrier wavelength, and is frequency dependent.

We will talk about both types of fading in this chapter, but with more emphasis on the latter. Large-scale fading is more relevant to issues such as cell-site planning. Small-scale multipath fading is more relevant to the design of reliable and efficient communication systems – the focus of this book.

We start with the physical modeling of the wireless channel in terms of electromagnetic waves. We then derive an input/output linear time-varying model for the channel, and define some important physical parameters. Finally, we introduce a few statistical models of the channel variation over time and over frequency.

2.1 Physical modeling for wireless channels

Wireless channels operate through electromagnetic radiation from the transmitter to the receiver. In principle, one could solve the electromagnetic field equations, in conjunction with the transmitted signal, to find the

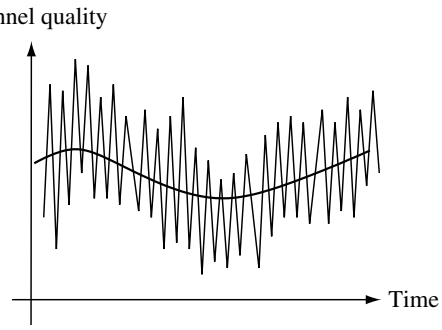

Figure 2.1 Channel quality varies over multiple time-scales. At a slow scale, channel varies due to large-scale fading effects. At a fast scale, channel varies due to multipath effects.

electromagnetic field impinging on the receiver antenna. This would have to be done taking into account the obstructions caused by ground, buildings, vehicles, etc. in the vicinity of this electromagnetic wave.[1]

Cellular communication in the USA is limited by the Federal Communication Commission (FCC), and by similar authorities in other countries, to one of three frequency bands, one around 0.9 GHz, one around 1.9 GHz, and one around 5.8 GHz. The wavelength λ of electromagnetic radiation at any given frequency f is given by $\lambda = c/f$, where $c = 3 \times 10^8$ m/s is the speed of light. The wavelength in these cellular bands is thus a fraction of a meter, so to calculate the electromagnetic field at a receiver, the locations of the receiver and the obstructions would have to be known within sub-meter accuracies. The electromagnetic field equations are therefore too complex to solve, especially on the fly for mobile users. Thus, we have to ask what we really need to know about these channels, and what approximations might be reasonable.

One of the important questions is where to choose to place the base-stations, and what range of power levels are then necessary on the downlink and uplink channels. To some extent this question must be answered experimentally, but it certainly helps to have a sense of what types of phenomena to expect. Another major question is what types of modulation and detection techniques look promising. Here again, we need a sense of what types of phenomena to expect. To address this, we will construct stochastic models of the channel, assuming that different channel behaviors appear with different probabilities, and change over time (with specific stochastic properties). We will return to the question of why such stochastic models are appropriate, but for now we simply want to explore the gross characteristics of these channels. Let us start by looking at several over-idealized examples.

[1] By obstructions, we mean not only objects in the line-of-sight between transmitter and receiver, but also objects in locations that cause non-negligible changes in the electromagnetic field at the receiver; we shall see examples of such obstructions later.

2.1.1 Free space, fixed transmit and receive antennas

First consider a fixed antenna radiating into free space. In the far field,[2] the electric field and magnetic field at any given location are perpendicular both to each other and to the direction of propagation from the antenna. They are also proportional to each other, so it is sufficient to know only one of them (just as in wired communication, where we view a signal as simply a voltage waveform or a current waveform). In response to a transmitted sinusoid $\cos 2\pi ft$, we can express the electric far field at time t as

$$E(f, t, (r, \theta, \psi)) = \frac{\alpha_s(\theta, \psi, f) \cos 2\pi f(t - r/c)}{r}. \tag{2.1}$$

Here, (r, θ, ψ) represents the point $\mathbf{u}$ in space at which the electric field is being measured, where r is the distance from the transmit antenna to $\mathbf{u}$ and where (θ, ψ) represents the vertical and horizontal angles from the antenna to $\mathbf{u}$ respectively. The constant c is the speed of light, and $\alpha_s(\theta, \psi, f)$ is the radiation pattern of the sending antenna at frequency f in the direction (θ, ψ); it also contains a scaling factor to account for antenna losses. Note that the phase of the field varies with fr/c, corresponding to the delay caused by the radiation traveling at the speed of light.

We are not concerned here with actually finding the radiation pattern for any given antenna, but only with recognizing that antennas have radiation patterns, and that the free space far field behaves as above.

It is important to observe that, as the distance r increases, the electric field decreases as r^{-1} and thus the power per square meter in the free space wave decreases as r^{-2}. This is expected, since if we look at concentric spheres of increasing radius r around the antenna, the total power radiated through the sphere remains constant, but the surface area increases as r^2. Thus, the power per unit area must decrease as r^{-2}. We will see shortly that this r^{-2} reduction of power with distance is often not valid when there are obstructions to free space propagation.

Next, suppose there is a fixed receive antenna at the location $\mathbf{u} = (r, \theta, \psi)$. The received waveform (in the absence of noise) in response to the above transmitted sinusoid is then

$$E_r(f, t, \mathbf{u}) = \frac{\alpha(\theta, \psi, f) \cos 2\pi f(t - r/c)}{r}, \tag{2.2}$$

where $\alpha(\theta, \psi, f)$ is the product of the antenna patterns of transmit and receive antennas in the given direction. Our approach to (2.2) is a bit odd since we started with the free space field at $\mathbf{u}$ in the absence of an antenna. Placing a

[2] The far field is the field sufficiently far away from the antenna so that (2.1) is valid. For cellular systems, it is a safe assumption that the receiver is in the far field.

receive antenna there changes the electric field in the vicinity of $\mathbf{u}$, but this is taken into account by the antenna pattern of the receive antenna.

Now suppose, for the given $\mathbf{u}$, that we define

$$H(f) := \frac{\alpha(\theta, \psi, f)\mathrm{e}^{-\mathrm{j}2\pi fr/c}}{r}. \tag{2.3}$$

We then have $E_{\mathrm{r}}(f, t, \mathbf{u}) = \Re\left[H(f)\mathrm{e}^{\mathrm{j}2\pi ft}\right]$. We have not mentioned it yet, but (2.1) and (2.2) are both linear in the input. That is, the received field (waveform) at $\mathbf{u}$ in response to a weighted sum of transmitted waveforms is simply the weighted sum of responses to those individual waveforms. Thus, $H(f)$ is the system function for an LTI (linear time-invariant) channel, and its inverse Fourier transform is the impulse response. The need for understanding electromagnetism is to determine what this system function is. We will find in what follows that linearity is a good assumption for all the wireless channels we consider, but that the time invariance does not hold when either the antennas or obstructions are in relative motion.

2.1.2 Free space, moving antenna

Next consider the fixed antenna and free space model above with a receive antenna that is moving with speed v in the direction of increasing distance from the transmit antenna. That is, we assume that the receive antenna is at a moving location described as $\mathbf{u}(t) = (r(t), \theta, \psi)$ with $r(t) = r_0 + vt$. Using (2.1) to describe the free space electric field at the moving point $\mathbf{u}(t)$ (for the moment with no receive antenna), we have

$$E(f, t, (r_0 + vt, \theta, \psi)) = \frac{\alpha_{\mathrm{s}}(\theta, \psi, f)\cos 2\pi f(t - r_0/c - vt/c)}{r_0 + vt}. \tag{2.4}$$

Note that we can rewrite $f(t - r_0/c - vt/c)$ as $f(1 - v/c)t - fr_0/c$. Thus, the sinusoid at frequency f has been converted to a sinusoid of frequency $f(1 - v/c)$; there has been a *Doppler shift* of $-fv/c$ due to the motion of the observation point.[3] Intuitively, each successive crest in the transmitted sinusoid has to travel a little further before it gets observed at the moving observation point. If the antenna is now placed at $\mathbf{u}(t)$, and the change of field due to the antenna presence is again represented by the receive antenna pattern, the received waveform, in analogy to (2.2), is

$$E_{\mathrm{r}}(f, t, (r_0 + vt, \theta, \psi)) = \frac{\alpha(\theta, \psi, f)\cos 2\pi f[(1 - v/c)t - r_0/c]}{r_0 + vt}. \tag{2.5}$$

[3] The reader should be familiar with the Doppler shift associated with moving cars. When an ambulance is rapidly moving toward us we hear a higher frequency siren. When it passes us we hear a rapid shift toward a lower frequency.

This channel cannot be represented as an LTI channel. If we ignore the time-varying attenuation in the denominator of (2.5), however, we can represent the channel in terms of a system function followed by translating the frequency f by the Doppler shift $-fv/c$. It is important to observe that the amount of shift depends on the frequency f. We will come back to discussing the importance of this Doppler shift and of the time-varying attenuation after considering the next example.

The above analysis does not depend on whether it is the transmitter or the receiver (or both) that are moving. So long as $r(t)$ is interpreted as the distance between the antennas (and the relative orientations of the antennas are constant), (2.4) and (2.5) are valid.

2.1.3 Reflecting wall, fixed antenna

Consider Figure 2.2 in which there is a fixed antenna transmitting the sinusoid $\cos 2\pi ft$, a fixed receive antenna, and a single perfectly reflecting large fixed wall. We assume that in the absence of the receive antenna, the electromagnetic field at the point where the receive antenna will be placed is the sum of the free space field coming from the transmit antenna plus a reflected wave coming from the wall. As before, in the presence of the receive antenna, the perturbation of the field due to the antenna is represented by the antenna pattern. An additional assumption here is that the presence of the receive antenna does not appreciably affect the plane wave impinging on the wall. In essence, what we have done here is to approximate the solution of Maxwell's equations by a method called *ray tracing*. The assumption here is that the received waveform can be approximated by the sum of the free space wave from the transmitter plus the reflected free space waves from each of the reflecting obstacles.

In the present situation, if we assume that the wall is very large, the reflected wave at a given point is the same (except for a sign change[4]) as the free space wave that would exist on the opposite side of the wall if the wall were not present (see Figure 2.3). This means that the reflected wave from the wall has the intensity of a free space wave at a distance equal to the distance to the wall and then

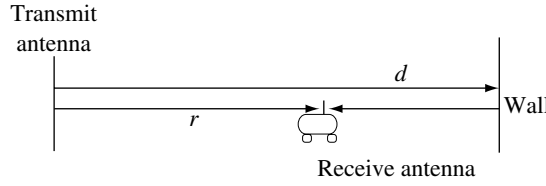

Figure 2.2 Illustration of a direct path and a reflected path.

[4] By basic electromagnetics, this sign change is a consequence of the fact that the electric field is parallel to the plane of the wall for this example.

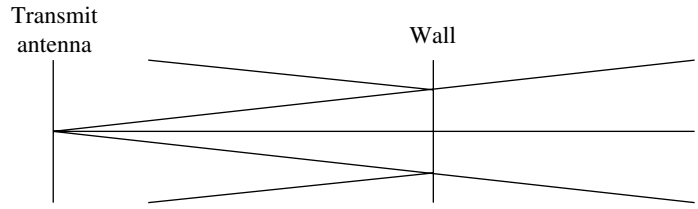

Figure 2.3 Relation of reflected wave to wave without wall.

back to the receive antenna, i.e., $2d - r$. Using (2.2) for both the direct and the reflected wave, and assuming the same antenna gain α for both waves, we get

$$E_{\mathrm{r}}(f,t) = \frac{\alpha \cos 2\pi f(t - r/c)}{r} - \frac{\alpha \cos 2\pi f(t - (2d - r)/c)}{2d - r}. \tag{2.6}$$

The received signal is a superposition of two waves, both of frequency f. The phase difference between the two waves is

$$\Delta\theta = \left(\frac{2\pi f(2d - r)}{c} + \pi\right) - \left(\frac{2\pi fr}{c}\right) = \frac{4\pi f}{c}(d - r) + \pi. \tag{2.7}$$

When the phase difference is an integer multiple of 2π, the two waves add *constructively*, and the received signal is strong. When the phase difference is an odd integer multiple of π, the two waves add *destructively*, and the received signal is weak. As a function of r, this translates into a spatial pattern of constructive and destructive interference of the waves. The distance from a peak to a valley is called the *coherence distance*:

$$\boxed{\Delta x_{\mathrm{c}} := \frac{\lambda}{4},} \tag{2.8}$$

where $\lambda := c/f$ is the wavelength of the transmitted sinusoid. At distances much smaller than Δx_{c}, the received signal at a particular time does not change appreciably.

The constructive and destructive interference pattern also depends on the frequency f: for a fixed r, if f changes by

$$\frac{1}{2}\left(\frac{2d - r}{c} - \frac{r}{c}\right)^{-1}, \tag{2.9}$$

we move from a peak to a valley. The quantity

$$\boxed{T_{\mathrm{d}} := \frac{2d - r}{c} - \frac{r}{c}} \tag{2.10}$$

is called the *delay spread* of the channel: it is the difference between the propagation delays along the two signal paths. The constructive and destructive interference pattern does not change appreciably if the frequency changes by an amount much smaller than $1/T_{\mathrm{d}}$. This parameter is called the *coherence bandwidth*.

2.1.4 Reflecting wall, moving antenna

Suppose the receive antenna is now moving at a velocity v (Figure 2.4). As it moves through the pattern of constructive and destructive interference created by the two waves, the strength of the received signal increases and decreases. This is the phenomenon of *multipath fading*. The time taken to travel from a peak to a valley is $c/(4fv)$: this is the time-scale at which the fading occurs, and it is called the *coherence time* of the channel.

An equivalent way of seeing this is in terms of the Doppler shifts of the direct and the reflected waves. Suppose the receive antenna is at location r_0 at time 0. Taking $r = r_0 + vt$ in (2.6), we get

$$E_r(f,t) = \frac{\alpha \cos 2\pi f[(1-v/c)t - r_0/c]}{r_0 + vt} - \frac{\alpha \cos 2\pi f[(1+v/c)t + (r_0 - 2d)/c]}{2d - r_0 - vt}. \quad (2.11)$$

The first term, the direct wave, is a sinusoid at frequency $f(1-v/c)$, experiencing a Doppler shift $D_1 := -fv/c$. The second is a sinusoid at frequency $f(1+v/c)$, with a Doppler shift $D_2 := +fv/c$. The parameter

$$\boxed{D_s := D_2 - D_1} \quad (2.12)$$

is called the *Doppler spread*. For example, if the mobile is moving at 60 km/h and $f = 900$ MHz, the Doppler spread is 100 Hz. The role of the Doppler spread can be visualized most easily when the mobile is much closer to the wall than to the transmit antenna. In this case the attenuations are roughly the same for both paths, and we can approximate the denominator of the second term by $r = r_0 + vt$. Then, combining the two sinusoids, we get

$$E_r(f,t) \approx \frac{2\alpha \sin 2\pi f\,[vt/c + (r_0 - d)/c] \sin 2\pi f[t - d/c]}{r_0 + vt}. \quad (2.13)$$

This is the product of two sinusoids, one at the input frequency f, which is typically of the order of GHz, and the other one at $fv/c = D_s/2$, which might be of the order of 50 Hz. Thus, the response to a sinusoid at f is another sinusoid at f with a time-varying envelope, with peaks going to zeros around every 5 ms (Figure 2.5). The envelope is at its widest when the mobile is at a peak of the

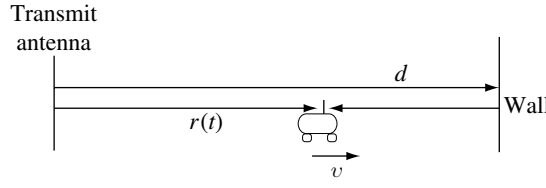

Figure 2.4 Illustration of a direct path and a reflected path.

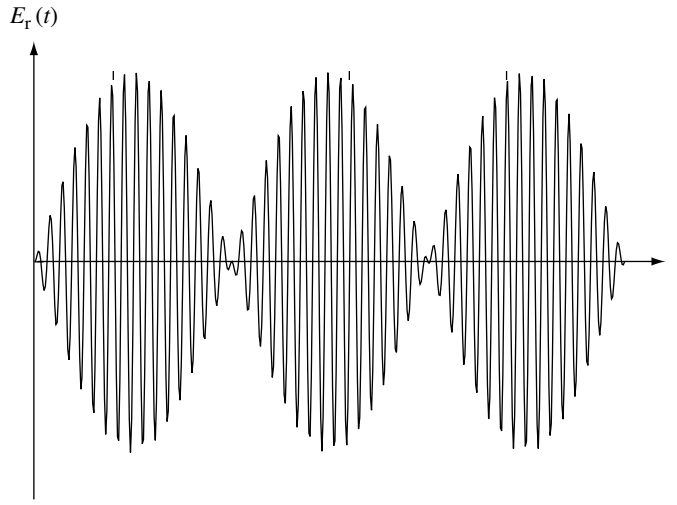

Figure 2.5 The received waveform oscillating at frequency f with a slowly varying envelope at frequency $D_s/2$.

interference pattern and at its narrowest when the mobile is at a valley. Thus, the Doppler spread determines the rate of traversal across the interference pattern and is inversely proportional to the coherence time of the channel.

We now see why we have partially ignored the denominator terms in (2.11) and (2.13). When the difference in the length between two paths changes by a quarter wavelength, the phase difference between the responses on the two paths changes by $\pi/2$, which causes a very significant change in the overall received amplitude. Since the carrier wavelength is very small relative to the path lengths, the time over which this phase effect causes a significant change is far smaller than the time over which the denominator terms cause a significant change. The effect of the phase changes is of the order of milliseconds, whereas the effect of changes in the denominator is of the order of seconds or minutes. In terms of modulation and detection, the time-scales of interest are in the range of milliseconds and less, and the denominators are effectively constant over these periods.

The reader might notice that we are constantly making approximations in trying to understand wireless communication, much more so than for wired communication. This is partly because wired channels are typically time-invariant over a very long time-scale, while wireless channels are typically time-varying, and appropriate models depend very much on the time-scales of interest. For wireless systems, the most important issue is what approximations to make. Thus, it is important to understand these modeling issues thoroughly.

2.1.5 Reflection from a ground plane

Consider a transmit and a receive antenna, both above a plane surface such as a road (Figure 2.6). When the horizontal distance r between the antennas becomes very large relative to their vertical displacements from the ground

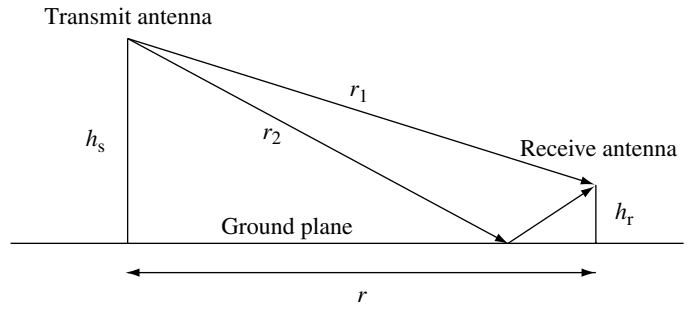

Figure 2.6 Illustration of a direct path and a reflected path off a ground plane.

plane (i.e., height), a very surprising thing happens. In particular, the difference between the direct path length and the reflected path length goes to zero as r^{-1} with increasing r (Exercise 2.5). When r is large enough, this difference between the path lengths becomes small relative to the wavelength c/f. Since the sign of the electric field is reversed on the reflected path[5], these two waves start to cancel each other out. The electric wave at the receiver is then attenuated as r^{-2}, and the received power decreases as r^{-4}. This situation is particularly important in rural areas where base-stations tend to be placed on roads.

2.1.6 Power decay with distance and shadowing

The previous example with reflection from a ground plane suggests that the received power can decrease with distance faster than r^{-2} in the presence of disturbances to free space. In practice, there are several obstacles between the transmitter and the receiver and, further, the obstacles might also absorb some power while scattering the rest. Thus, one expects the power decay to be considerably faster than r^{-2}. Indeed, empirical evidence from experimental field studies suggests that while power decay near the transmitter is like r^{-2}, at large distances the power can even decay *exponentially* with distance.

The ray tracing approach used so far provides a high degree of numerical accuracy in determining the electric field at the receiver, but requires a precise physical model including the location of the obstacles. But here, we are only looking for the order of decay of power with distance and can consider an alternative approach. So we look for a model of the physical environment with the fewest parameters but one that still provides useful global information about the field properties. A simple probabilistic model with two parameters of the physical environment, the density of the obstacles and the fraction of energy each object absorbs, is developed in Exercise 2.6. With each obstacle

[5] This is clearly true if the electric field is parallel to the ground plane. It turns out that this is also true for arbitrary orientations of the electric field, as long as the ground is not a perfect conductor and the angle of incidence is small enough. The underlying electromagnetics is analyzed in Chapter 2 of Jakes [62].

absorbing the same fraction of the energy impinging on it, the model allows us to show that the power decays exponentially in distance at a rate that is proportional to the density of the obstacles.

With a limit on the transmit power (either at the base-station or at the mobile), the largest distance between the base-station and a mobile at which communication can reliably take place is called the *coverage* of the cell. For reliable communication, a minimal received power level has to be met and thus the fast decay of power with distance constrains cell coverage. On the other hand, rapid signal attenuation with distance is also helpful; it reduces the *interference* between adjacent cells. As cellular systems become more popular, however, the major determinant of cell size is the number of mobiles in the cell. In engineering jargon, the cell is said to be *capacity* limited instead of coverage limited. The size of cells has been steadily decreasing, and one talks of micro cells and pico cells as a response to this effect. With capacity limited cells, the inter-cell interference may be intolerably high. To alleviate the inter-cell interference, neighboring cells use different parts of the frequency spectrum, and frequency is reused at cells that are far enough. Rapid signal attenuation with distance allows frequencies to be reused at closer distances.

The density of obstacles between the transmit and receive antennas depends very much on the physical environment. For example, outdoor plains have very little by way of obstacles while indoor environments pose many obstacles. This randomness in the environment is captured by modeling the density of obstacles and their absorption behavior as random numbers; the overall phenomenon is called *shadowing*.[6] The effect of shadow fading differs from multipath fading in an important way. The duration of a shadow fade lasts for multiple seconds or minutes, and hence occurs at a much slower time-scale compared to multipath fading.

2.1.7 Moving antenna, multiple reflectors

Dealing with multiple reflectors, using the technique of ray tracing, is in principle simply a matter of modeling the received waveform as the sum of the responses from the different paths rather than just two paths. We have seen enough examples, however, to understand that finding the magnitudes and phases of these responses is no simple task. Even for the very simple large wall example in Figure 2.2, the reflected field calculated in (2.6) is valid only at distances from the wall that are small relative to the dimensions of the wall. At very large distances, the total power reflected from the wall is proportional to both d^{-2} and to the area of the cross section of the wall. The power reaching the receiver is proportional to $(d - r(t))^{-2}$. Thus, the power attenuation from transmitter to receiver (for the large distance case) is proportional to $(d(d - r(t)))^{-2}$ rather

[6] This is called shadowing because it is similar to the effect of clouds partly blocking sunlight.

than to $(2d - r(t))^{-2}$. This shows that ray tracing must be used with some caution. Fortunately, however, linearity still holds in these more complex cases.

Another type of reflection is known as *scattering* and can occur in the atmosphere or in reflections from very rough objects. Here there are a very large number of individual paths, and the received waveform is better modeled as an integral over paths with infinitesimally small differences in their lengths, rather than as a sum.

Knowing how to find the amplitude of the reflected field from each type of reflector is helpful in determining the coverage of a base-station (although ultimately experimentation is necessary). This is an important topic if our objective is trying to determine where to place base-stations. Studying this in more depth, however, would take us afield and too far into electromagnetic theory. In addition, we are primarily interested in questions of modulation, detection, multiple access, and network protocols rather than location of base-stations. Thus, we turn our attention to understanding the nature of the aggregate received waveform, given a representation for each reflected wave. This leads to modeling the input/output behavior of a channel rather than the detailed response on each path.

2.2 Input/output model of the wireless channel

We derive an input/output model in this section. We first show that the multipath effects can be modeled as a linear time-varying system. We then obtain a baseband representation of this model. The continuous-time channel is then sampled to obtain a discrete-time model. Finally we incorporate additive noise.

2.2.1 The wireless channel as a linear time-varying system

In the previous section we focused on the response to the sinusoidal input $\phi(t) = \cos 2\pi ft$. The received signal can be written as $\sum_i a_i(f, t)\phi(t - \tau_i(f, t))$, where $a_i(f, t)$ and $\tau_i(f, t)$ are respectively the overall attenuation and propagation delay at time t from the transmitter to the receiver on path i. The overall attenuation is simply the product of the attenuation factors due to the antenna pattern of the transmitter and the receiver, the nature of the reflector, as well as a factor that is a function of the distance from the transmitting antenna to the reflector and from the reflector to the receive antenna. We have described the channel effect at a particular frequency f. If we further assume that the $a_i(f, t)$ and the $\tau_i(f, t)$ do not depend on the frequency f, then we can use the principle of superposition to generalize the above input/output relation to an arbitrary input $x(t)$ with non-zero bandwidth:

$$y(t) = \sum_i a_i(t)x(t - \tau_i(t)). \tag{2.14}$$

In practice the attenuations and the propagation delays are usually slowly varying functions of frequency. These variations follow from the time-varying path lengths and also from frequency-dependent antenna gains. However, we are primarily interested in transmitting over bands that are narrow relative to the carrier frequency, and over such ranges we can omit this frequency dependence. It should however be noted that although the *individual* attenuations and delays are assumed to be independent of the frequency, the *overall* channel response can still vary with frequency due to the fact that different paths have different delays.

For the example of a perfectly reflecting wall in Figure 2.4, then,

$$a_1(t) = \frac{|\alpha|}{r_0 + vt}, \qquad a_2(t) = \frac{|\alpha|}{2d - r_0 - vt}, \tag{2.15}$$

$$\tau_1(t) = \frac{r_0 + vt}{c} - \frac{\angle\phi_1}{2\pi f}, \qquad \tau_2(t) = \frac{2d - r_0 - vt}{c} - \frac{\angle\phi_2}{2\pi f}, \tag{2.16}$$

where the first expression is for the direct path and the second for the reflected path. The term $\angle\phi_j$ here is to account for possible phase changes at the transmitter, reflector, and receiver. For the example here, there is a phase reversal at the reflector so we take $\phi_1 = 0$ and $\phi_2 = \pi$.

Since the channel (2.14) is linear, it can be described by the response $h(\tau, t)$ at time t to an impulse transmitted at time $t - \tau$. In terms of $h(\tau, t)$, the input/output relationship is given by

$$y(t) = \int_{-\infty}^{\infty} h(\tau, t)x(t - \tau)\,\mathrm{d}\tau. \tag{2.17}$$

Comparing (2.17) and (2.14), we see that the impulse response for the fading multipath channel is

$$h(\tau, t) = \sum_i a_i(t)\delta(\tau - \tau_i(t)). \tag{2.18}$$

This expression is really quite nice. It says that the effect of mobile users, arbitrarily moving reflectors and absorbers, and all of the complexities of solving Maxwell's equations, finally reduce to an input/output relation between transmit and receive antennas which is simply represented as the impulse response of a linear time-varying channel filter.

The effect of the Doppler shift is not immediately evident in this representation. From (2.16) for the single reflecting wall example, $\tau_i'(t) = v_i/c$ where v_i is the velocity with which the ith path length is increasing. Thus, the Doppler shift on the ith path is $-f\tau_i'(t)$.

In the special case when the transmitter, receiver and the environment are all stationary, the attenuations $a_i(t)$ and propagation delays $\tau_i(t)$ do not

depend on time t, and we have the usual linear time-invariant channel with an impulse response

$$h(\tau) = \sum_i a_i \delta(\tau - \tau_i). \tag{2.19}$$

For the time-varying impulse response $h(\tau, t)$, we can define a time-varying frequency response

$$H(f; t) := \int_{-\infty}^{\infty} h(\tau, t) \mathrm{e}^{-\mathrm{j}2\pi f\tau} \, \mathrm{d}\tau = \sum_i a_i(t) \mathrm{e}^{-\mathrm{j}2\pi f\tau_i(t)}. \tag{2.20}$$

In the special case when the channel is time-invariant, this reduces to the usual frequency response. One way of interpreting $H(f; t)$ is to think of the system as a slowly varying function of t with a frequency response $H(f; t)$ at each fixed time t. Corresponding, $h(\tau, t)$ can be thought of as the impulse response of the system at a fixed time t. This is a legitimate and useful way of thinking about many multipath fading channels, as the time-scale at which the channel varies is typically much longer than the delay spread (i.e., the amount of memory) of the impulse response at a fixed time. In the reflecting wall example in Section 2.1.4, the time taken for the channel to change significantly is of the order of milliseconds while the delay spread is of the order of microseconds. Fading channels which have this characteristic are sometimes called *underspread* channels.

2.2.2 Baseband equivalent model

In typical wireless applications, communication occurs in a passband $[f_\mathrm{c} - W/2, f_\mathrm{c} + W/2]$ of bandwidth W around a center frequency f_c, the spectrum having been specified by regulatory authorities. However, most of the processing, such as coding/decoding, modulation/demodulation, synchronization, etc., is actually done at the baseband. At the transmitter, the last stage of the operation is to "up-convert" the signal to the carrier frequency and transmit it via the antenna. Similarly, the first step at the receiver is to "down-convert" the RF (radio-frequency) signal to the baseband before further processing. Therefore from a communication system design point of view, it is most useful to have a baseband equivalent representation of the system. We first start with defining the baseband equivalent representation of signals.

Consider a real signal $s(t)$ with Fourier transform $S(f)$, band-limited in $[f_\mathrm{c} - W/2, f_\mathrm{c} + W/2]$ with $W < 2f_\mathrm{c}$. Define its *complex baseband equivalent* $s_\mathrm{b}(t)$ as the signal having Fourier transform:

$$S_\mathrm{b}(f) = \begin{cases} \sqrt{2}S(f + f_\mathrm{c}) & f + f_\mathrm{c} > 0, \\ 0 & f + f_\mathrm{c} \le 0. \end{cases} \tag{2.21}$$

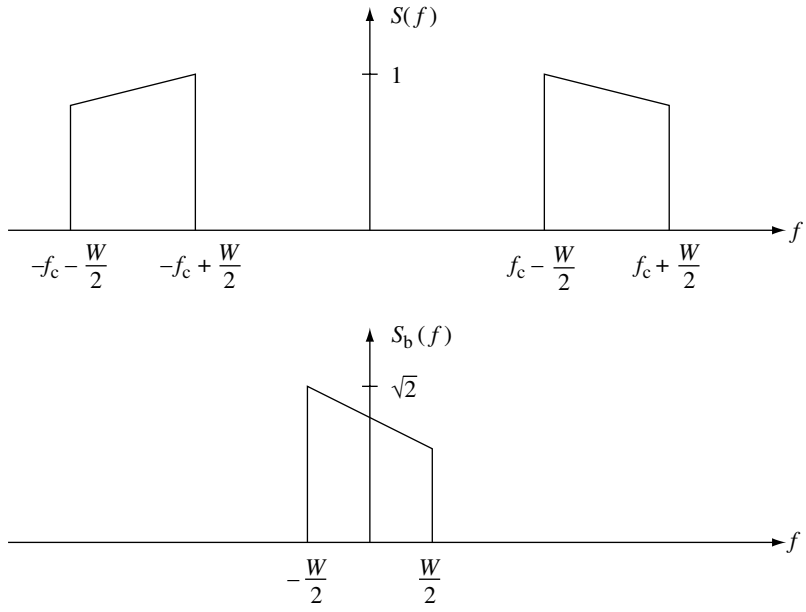

Figure 2.7 Illustration of the relationship between a passband spectrum *S(f)* and its baseband equivalent $S_b(f)$.

Since $s(t)$ is real, its Fourier transform satisfies $S(f) = S^*(-f)$, which means that $s_b(t)$ contains exactly the same information as $s(t)$. The factor of $\sqrt{2}$ is quite arbitrary but chosen to normalize the energies of $s_b(t)$ and $s(t)$ to be the same. Note that $s_b(t)$ is band-limited in $[-W/2, W/2]$. See Figure 2.7.

To reconstruct $s(t)$ from $s_b(t)$, we observe that

$$\sqrt{2}S(f) = S_b(f - f_c) + S_b^*(-f - f_c). \tag{2.22}$$

Taking inverse Fourier transforms, we get

$$s(t) = \frac{1}{\sqrt{2}}\left[s_b(t)e^{j2\pi f_c t} + s_b^*(t)e^{-j2\pi f_c t}\right] = \sqrt{2}\Re\left[s_b(t)e^{j2\pi f_c t}\right]. \tag{2.23}$$

In terms of real signals, the relationship between $s(t)$ and $s_b(t)$ is shown in Figure 2.8. The passband signal $s(t)$ is obtained by modulating $\Re[s_b(t)]$ by $\sqrt{2}\cos 2\pi f_c t$ and $\Im[s_b(t)]$ by $-\sqrt{2}\sin 2\pi f_c t$ and summing, to get $\sqrt{2}\Re\left[s_b(t)e^{j2\pi f_c t}\right]$ (up-conversion). The baseband signal $\Re[s_b(t)]$ (respectively $\Im[s_b(t)]$) is obtained by modulating $s(t)$ by $\sqrt{2}\cos 2\pi f_c t$ (respectively $-\sqrt{2}\sin 2\pi f_c t$) followed by ideal low-pass filtering at the baseband $[-W/2, W/2]$ (down-conversion).

Let us now go back to the multipath fading channel (2.14) with impulse response given by (2.18). Let $x_b(t)$ and $y_b(t)$ be the complex baseband equivalents of the transmitted signal $x(t)$ and the received signal $y(t)$, respectively. Figure 2.9 shows the system diagram from $x_b(t)$ to $y_b(t)$. This implementation of a passband communication system is known as *quadrature amplitude modulation* (QAM). The signal $\Re[x_b(t)]$ is sometimes called the

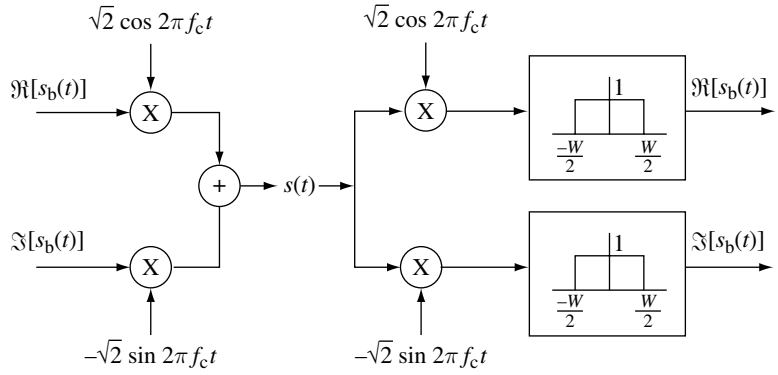

Figure 2.8 Illustration of upconversion from $s_b(t)$ to $s(t)$, followed by downconversion from $s(t)$ back to $s_b(t)$.

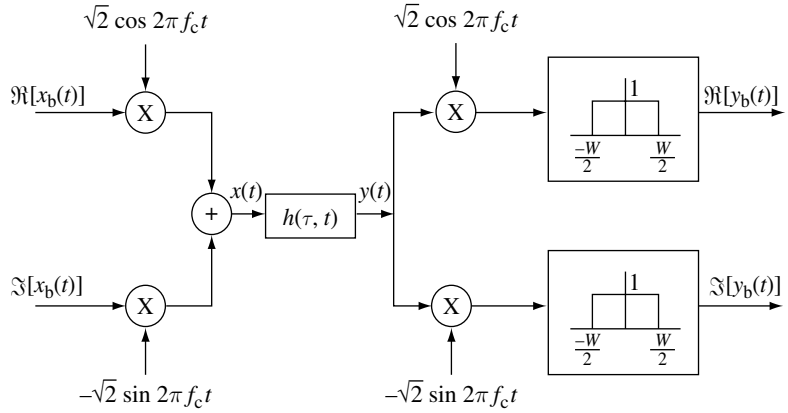

Figure 2.9 System diagram from the baseband transmitted signal $x_b(t)$ to the baseband received signal $y_b(t)$.

in-phase component I and $\Im[x_b(t)]$ the quadrature component Q (rotated by $\pi/2$). We now calculate the baseband equivalent channel. Substituting $x(t) = \sqrt{2}\Re[x_b(t)e^{j2\pi f_c t}]$ and $y(t) = \sqrt{2}\Re[y_b(t)e^{j2\pi f_c t}]$ into (2.14) we get

$$\begin{aligned}\Re[y_b(t)e^{j2\pi f_c t}] &= \sum_i a_i(t)\Re[x_b(t-\tau_i(t))e^{j2\pi f_c(t-\tau_i(t))}] \\ &= \Re\left[\left\{\sum_i a_i(t)x_b(t-\tau_i(t))e^{-j2\pi f_c\tau_i(t)}\right\}e^{j2\pi f_c t}\right]. \quad (2.24)\end{aligned}$$

Similarly, one can obtain (Exercise 2.13)

$$\Im[y_b(t)e^{j2\pi f_c t}] = \Im\left[\left\{\sum_i a_i(t)x_b(t-\tau_i(t))e^{-j2\pi f_c\tau_i(t)}\right\}e^{j2\pi f_c t}\right]. \quad (2.25)$$

Hence, the baseband equivalent channel is

$$y_b(t) = \sum_i a_i^b(t)x_b(t-\tau_i(t)), \quad (2.26)$$

where

$$a_i^{\mathrm{b}}(t) := a_i(t)\mathrm{e}^{-\mathrm{j}2\pi f_{\mathrm{c}}\tau_i(t)}. \tag{2.27}$$

The input/output relationship in (2.26) is also that of a linear time-varying system, and the baseband equivalent impulse response is

$$h_{\mathrm{b}}(\tau, t) = \sum_i a_i^{\mathrm{b}}(t)\delta(\tau - \tau_i(t)). \tag{2.28}$$

This representation is easy to interpret in the time domain, where the effect of the carrier frequency can be seen explicitly. The baseband output is the sum, over each path, of the delayed replicas of the baseband input. The magnitude of the ith such term is the magnitude of the response on the given path; this changes slowly, with significant changes occurring on the order of seconds or more. The phase is changed by $\pi/2$ (i.e., is changed significantly) when the delay on the path changes by $1/(4f_{\mathrm{c}})$, or equivalently, when the path length changes by a quarter wavelength, i.e., by $c/(4f_{\mathrm{c}})$. If the path length is changing at velocity v, the time required for such a phase change is $c/(4f_{\mathrm{c}}v)$. Recalling that the Doppler shift D at frequency f is fv/c, and noting that $f \approx f_{\mathrm{c}}$ for narrowband communication, the time required for a $\pi/2$ phase change is $1/(4D)$. For the single reflecting wall example, this is about 5 ms (assuming $f_{\mathrm{c}} = 900\,\mathrm{MHz}$ and $v = 60\,\mathrm{km/h}$). The phases of both paths are rotating at this rate but in opposite directions.

Note that the Fourier transform $H_{\mathrm{b}}(f; t)$ of $h_{\mathrm{b}}(\tau, t)$ for a fixed t is simply $H(f + f_{\mathrm{c}}; t)$, i.e., the frequency response of the original system (at a fixed t) shifted by the carrier frequency. This provides another way of thinking about the baseband equivalent channel.

2.2.3 A discrete-time baseband model

The next step in creating a useful channel model is to convert the continuous-time channel to a discrete-time channel. We take the usual approach of the sampling theorem. Assume that the input waveform is band-limited to W. The baseband equivalent is then limited to $W/2$ and can be represented as

$$x_{\mathrm{b}}(t) = \sum_n x[n]\mathrm{sinc}(Wt - n), \tag{2.29}$$

where $x[n]$ is given by $x_{\mathrm{b}}(n/W)$ and $\mathrm{sinc}(t)$ is defined as

$$\mathrm{sinc}(t) := \frac{\sin(\pi t)}{\pi t}. \tag{2.30}$$

This representation follows from the sampling theorem, which says that any waveform band-limited to $W/2$ can be expanded in terms of the orthogonal

basis $\{\text{sinc}(Wt-n)\}_n$, with coefficients given by the samples (taken uniformly at integer multiples of $1/W$).

Using (2.26), the baseband output is given by

$$y_{\text{b}}(t) = \sum_n x[n] \sum_i a_i^{\text{b}}(t)\text{sinc}(Wt - W\tau_i(t) - n). \tag{2.31}$$

The sampled outputs at multiples of $1/W$, $y[m] := y_{\text{b}}(m/W)$, are then given by

$$y[m] = \sum_n x[n] \sum_i a_i^{\text{b}}(m/W)\text{sinc}[m - n - \tau_i(m/W)W]. \tag{2.32}$$

The sampled output $y[m]$ can equivalently be thought of as the projection of the waveform $y_{\text{b}}(t)$ onto the waveform $W\text{sinc}(Wt-m)$. Let $\ell := m-n$. Then

$$y[m] = \sum_\ell x[m-\ell] \sum_i a_i^{\text{b}}(m/W)\text{sinc}[\ell - \tau_i(m/W)W]. \tag{2.33}$$

By defining

$$\boxed{h_\ell[m] := \sum_i a_i^{\text{b}}(m/W)\text{sinc}[\ell - \tau_i(m/W)W],} \tag{2.34}$$

(2.33) can be written in the simple form

$$y[m] = \sum_\ell h_\ell[m]\, x[m-\ell]. \tag{2.35}$$

We denote $h_\ell[m]$ as the ℓth (complex) channel filter tap at time m. Its value is a function of mainly the gains $a_i^{\text{b}}(t)$ of the paths, whose delays $\tau_i(t)$ are close to ℓ/W (Figure 2.10). In the special case where the gains $a_i^{\text{b}}(t)$ and the delays $\tau_i(t)$ of the paths are time-invariant, (2.34) simplifies to

$$h_\ell = \sum_i a_i^{\text{b}}\ \text{sinc}[\ell - \tau_i W], \tag{2.36}$$

and the channel is linear time-invariant. The ℓth tap can be interpreted as the sample (ℓ/W)th of the low-pass filtered baseband channel response $h_{\text{b}}(\tau)$ (cf. (2.19)) convolved with $\text{sinc}(W\tau)$.

We can interpret the sampling operation as modulation and demodulation in a communication system. At time n, we are modulating the complex symbol $x[m]$ (in-phase plus quadrature components) by the sinc pulse before the up-conversion. At the receiver, the received signal is sampled at times m/W

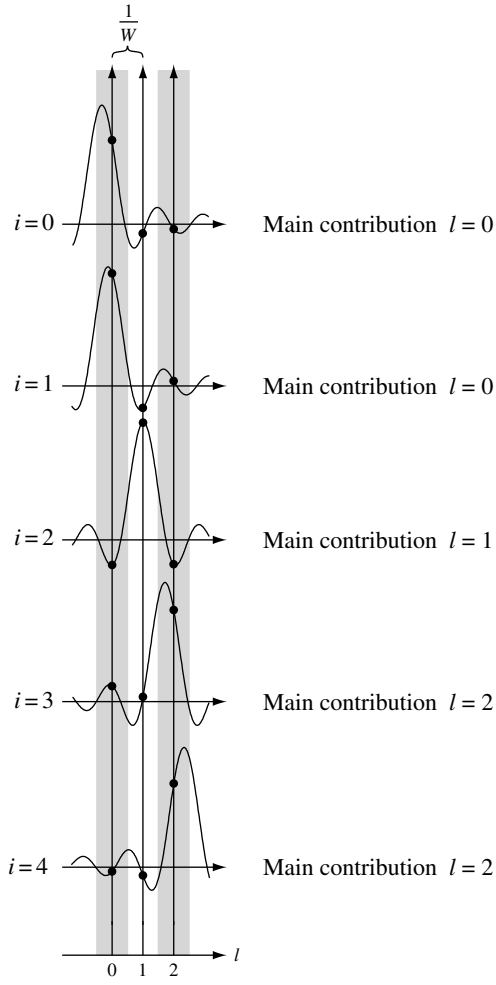

Figure 2.10 Due to the decay of the sinc function, the ith path contributes most significantly to the ℓth tap if its delay falls in the window $[\ell/W - 1/(2W), \ell/W + 1/(2W)]$.

at the output of the low-pass filter. Figure 2.11 shows the complete system. In practice, other transmit pulses, such as the raised cosine pulse, are often used in place of the sinc pulse, which has rather poor time-decay property and tends to be more susceptible to timing errors. This necessitates sampling at the Nyquist sampling rate, but does not alter the essential nature of the model. Hence we will confine to Nyquist sampling.

Due to the Doppler spread, the bandwidth of the output $y_b(t)$ is generally slightly larger than the bandwidth $W/2$ of the input $x_b(t)$, and thus the output samples $\{y[m]\}$ do not fully represent the output waveform. This problem is usually ignored in practice, since the Doppler spread is small (of the order of tens to hundreds of Hz) compared to the bandwidth W. Also, it is very convenient for the sampling rate of the input and output to be the same. Alternatively, it would be possible to sample the output at twice the rate of the input. This would recapture all the information in the received waveform.

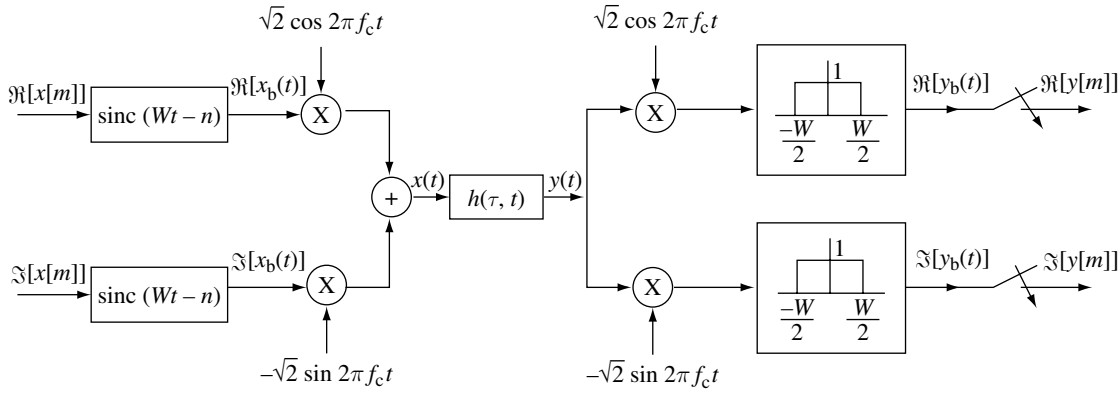

Figure 2.11 System diagram from the baseband transmitted symbol $x[m]$ to the baseband sampled received signal $y[m]$.

The number of taps would be almost doubled because of the reduced sample interval, but it would typically be somewhat less than doubled since the representation would not spread the path delays so much.

Discussion 2.1 Degrees of freedom

The symbol $x[m]$ is the mth sample of the transmitted signal; there are W samples per second. Each symbol is a complex number; we say that it represents one (complex) *dimension* or *degree of freedom*. The continuous-time signal $x(t)$ of duration one second corresponds to W discrete symbols; thus we could say that the band-limited, continuous-time signal has W degrees of freedom, per second.

The mathematical justification for this interpretation comes from the following important result in communication theory: the signal space of complex continuous-time signals of duration T which have most of their energy within the frequency band $[-W/2, W/2]$ has dimension approximately WT. (A precise statement of this result is in standard communication theory text/books; see Section 5.3 of [148] for example.) This result reinforces our interpretation that a continuous-time signal with bandwidth W can be represented by W complex dimensions per second.

The received signal $y(t)$ is also band-limited to approximately W (due to the Doppler spread, the bandwidth is slightly larger than W) and has W complex dimensions per second. From the point of view of communication over the channel, the *received* signal space is what matters because it dictates the number of different signals which can be reliably distinguished at the receiver. Thus, we define the *degrees of freedom of the channel* to be the dimension of the received signal space, and whenever we refer to the signal space, we implicitly mean the received signal space unless stated otherwise.

2.2.4 Additive white noise

As a last step, we include additive noise in our input/output model. We make the standard assumption that $w(t)$ is zero-mean additive white Gaussian noise (AWGN) with power spectral density $N_0/2$ (i.e., $E[w(0)w(t)] = (N_0/2)\delta(t)$. The model (2.14) is now modified to be

$$y(t) = \sum_i a_i(t)x(t - \tau_i(t)) + w(t). \tag{2.37}$$

See Figure 2.12. The discrete-time baseband-equivalent model (2.35) now becomes

$$y[m] = \sum_\ell h_\ell[m]x[m - \ell] + w[m], \tag{2.38}$$

where $w[m]$ is the low-pass filtered noise at the sampling instant m/W. Just like the signal, the white noise $w(t)$ is down-converted, filtered at the baseband and ideally sampled. Thus, it can be verified (Exercise 2.11) that

$$\Re(w[m]) = \int_{-\infty}^{\infty} w(t)\psi_{m,1}(t)\mathrm{d}t, \tag{2.39}$$

$$\Im(w[m]) = \int_{-\infty}^{\infty} w(t)\psi_{m,2}(t)\mathrm{d}t, \tag{2.40}$$

where

$$\begin{aligned} \psi_{m,1}(t) &:= \sqrt{2W}\cos(2\pi f_c t)\mathrm{sinc}(Wt - m), \\ \psi_{m,2}(t) &:= -\sqrt{2W}\sin(2\pi f_c t)\mathrm{sinc}(Wt - m). \end{aligned} \tag{2.41}$$

It can further be shown that $\{\psi_{m,1}(t), \psi_{m,2}(t)\}_m$ forms an *orthonormal set* of waveforms, i.e., the waveforms are orthogonal to each other (Exercise 2.12). In Appendix A we review the definition and basic properties of white Gaussian random *vectors* (i.e., vectors whose components are independent and identically distributed (i.i.d.) Gaussian random variables). A key property is that the projections of a white Gaussian random vector onto any orthonormal vectors are independent and identically distributed Gaussian random variables. Heuristically, one can think of continuous-time Gaussian white noise as an infinite-dimensional white random vector and the above property carries through: the projections onto orthogonal waveforms are uncorrelated and hence independent. Hence the discrete-time noise process $\{w[m]\}$ is white, i.e., independent over time; moreover, the real and imaginary components are i.i.d. Gaussians with variances $N_0/2$. A complex Gaussian random variable X whose real and imaginary components are i.i.d. satisfies a *circular symmetry* property: $\mathrm{e}^{\mathrm{j}\phi}X$ has the same distribution as X for any ϕ. We shall call such a random variable *circular symmetric complex*

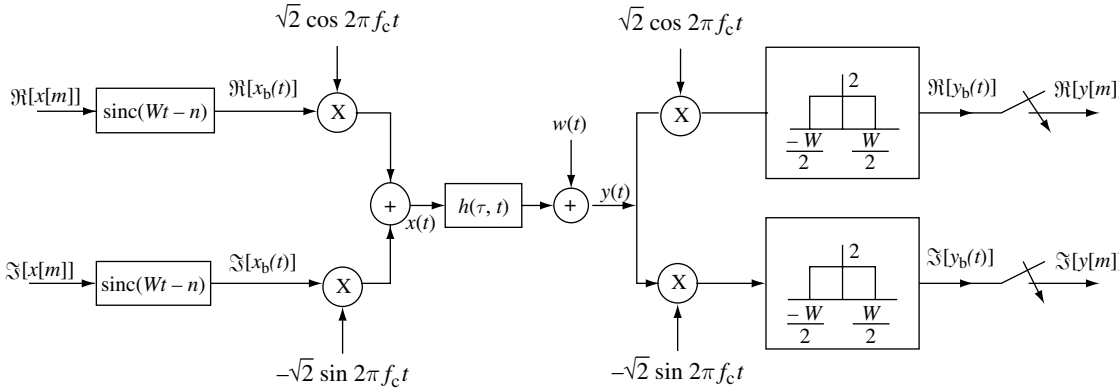

Figure 2.12 A complete system diagram.

Gaussian, denoted by $\mathcal{CN}(0, \sigma^2)$, where $\sigma^2 = E[|X|^2]$. The concept of circular symmetry is discussed further in Section A.1.3 of Appendix A.

The assumption of AWGN essentially means that we are assuming that the primary source of the noise is at the receiver or is radiation impinging on the receiver that is independent of the paths over which the signal is being received. This is normally a very good assumption for most communication situations.

2.3 Time and frequency coherence

2.3.1 Doppler spread and coherence time

An important channel parameter is the time-scale of the variation of the channel. How fast do the taps $h_\ell[m]$ vary as a function of time m? Recall that

$$\begin{aligned} h_\ell[m] &= \sum_i a_i^{\mathrm{b}}(m/W)\mathrm{sinc}[\ell - \tau_i(m/W)W] \\ &= \sum_i a_i(m/W)\mathrm{e}^{-\mathrm{j}2\pi f_c \tau_i(m/W)}\mathrm{sinc}[\ell - \tau_i(m/W)W]. \end{aligned} \tag{2.42}$$

Let us look at this expression term by term. From Section 2.2.2 we gather that significant changes in a_i occur over periods of seconds or more. Significant changes in the phase of the ith path occur at intervals of $1/(4D_i)$, where $D_i = f_c\tau_i'(t)$ is the Doppler shift for that path. When the different paths contributing to the ℓth tap have different Doppler shifts, the magnitude of $h_\ell[m]$ changes significantly. This is happening at the time-scale inversely proportional to the largest difference between the Doppler shifts, the *Doppler spread* D_s:

$$\boxed{D_s := \max_{i,j} f_c|\tau_i'(t) - \tau_j'(t)|,} \tag{2.43}$$

where the maximum is taken over all the paths that contribute significantly to a tap.[7] Typical intervals for such changes are on the order of 10 ms. Finally, changes in the sinc term of (2.42) due to the time variation of each $\tau_i(t)$ are proportional to the bandwidth, whereas those in the phase are proportional to the carrier frequency, which is typically much larger. Essentially, it takes much longer for a path to move from one tap to the next than for its phase to change significantly. Thus, the fastest changes in the filter taps occur because of the phase changes, and these are significant over delay changes of $1/(4D_s)$.

The coherence time T_c of a wireless channel is defined (in an order of magnitude sense) as the interval over which $h_\ell[m]$ changes significantly as a function of m. What we have found, then, is the important relation

$$\boxed{T_c = \frac{1}{4D_s}.} \tag{2.44}$$

This is a somewhat imprecise relation, since the largest Doppler shifts may belong to paths that are too weak to make a difference. We could also view a phase change of $\pi/4$ to be significant, and thus replace the factor of 4 above by 8. Many people instead replace the factor of 4 by 1. The important thing is to recognize that the major effect in determining time coherence is the Doppler spread, and that the relationship is reciprocal; the larger the Doppler spread, the smaller the time coherence.

In the wireless communication literature, channels are often categorized as *fast fading* and *slow fading*, but there is little consensus on what these terms mean. In this book, we will call a channel fast fading if the coherence time T_c is much shorter than the delay requirement of the application, and slow fading if T_c is longer. The operational significance of this definition is that, in a fast fading channel, one can transmit the coded symbols over multiple fades of the channel, while in a slow fading channel, one cannot. Thus, whether a channel is fast or slow fading depends not only on the environment but also on the application; voice, for example, typically has a short delay requirement of less than 100 ms, while some types of data applications can have a laxer delay requirement.

2.3.2 Delay spread and coherence bandwidth

Another important general parameter of a wireless system is the multipath delay spread, T_d, defined as the difference in propagation time between the

[7] The Doppler spread can in principle be different for different taps. Exercise 2.10 explores this possibility.

longest and shortest path, counting only the paths with significant energy. Thus,

$$\boxed{T_{\mathrm{d}} := \max_{i,\,j} |\tau_i(t) - \tau_j(t)|.} \tag{2.45}$$

This is defined as a function of t, but we regard it as an order of magnitude quantity, like the time coherence and Doppler spread. If a cell or LAN has a linear extent of a few kilometers or less, it is very unlikely to have path lengths that differ by more than 300 to 600 meters. This corresponds to path delays of one or two microseconds. As cells become smaller due to increased cellular usage, T_{d} also shrinks. As was already mentioned, typical wireless channels are underspread, which means that the delay spread T_{d} is much smaller than the coherence time T_{c}.

The bandwidths of cellular systems range between several hundred kilohertz and several megahertz, and thus, for the above multipath delay spread values, all the path delays in (2.34) lie within the peaks of two or three sinc functions; more often, they lie within a single peak. Adding a few extra taps to each channel filter because of the slow decay of the sinc function, we see that cellular channels can be represented with at most four or five channel filter taps. On the other hand, there is a recent interest in *ultra-wideband* (UWB) communication, operating from 3.1 to 10.6 GHz. These channels can have up to a few hundred taps.

When we study modulation and detection for cellular systems, we shall see that the receiver must estimate the values of these channel filter taps. The taps are estimated via transmitted and received waveforms, and thus the receiver makes no explicit use of (and usually does not have) any information about individual path delays and path strengths. This is why we have not studied the details of propagation over multiple paths with complicated types of reflection mechanisms. All we really need is the aggregate values of gross physical mechanisms such as Doppler spread, coherence time, and multipath spread.

The delay spread of the channel dictates its *frequency coherence*. Wireless channels change both in time and frequency. The time coherence shows us how quickly the channel changes in time, and similarly, the frequency coherence shows how quickly it changes in frequency. We first understood about channels changing in time, and correspondingly about the duration of fades, by studying the simple example of a direct path and a single reflected path. That same example also showed us how channels change with frequency. We can see this in terms of the frequency response as well.

Recall that the frequency response at time t is

$$H(f; t) = \sum_i a_i(t) \mathrm{e}^{-\mathrm{j}2\pi f \tau_i(t)}. \tag{2.46}$$

The contribution due to a particular path has a phase linear in f. For multiple paths, there is a differential phase, $2\pi f(\tau_i(t) - \tau_k(t))$. This differential

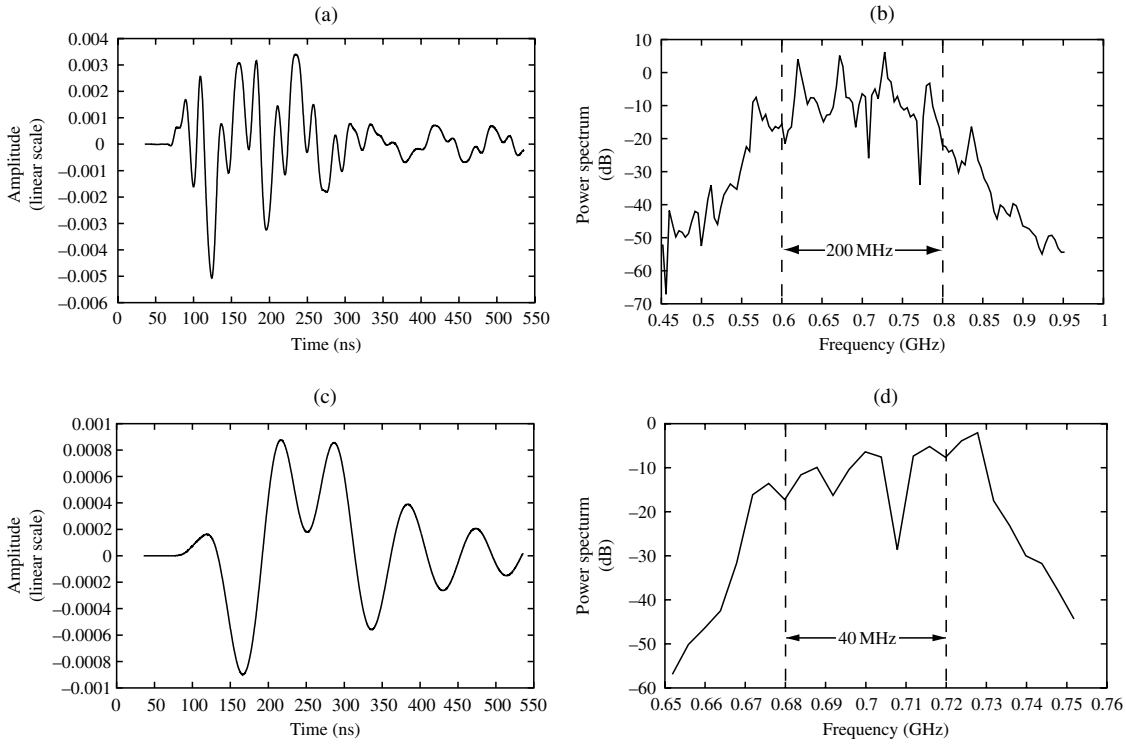

Figure 2.13 (a) A channel over 200 MHz is frequency-selective, and the impulse response has many taps. (b) The spectral content of the same channel. (c) The same channel over 40 MHz is flatter, and has for fewer taps. (d) The spectral contents of the same channel, limited to 40 MHz bandwidth. At larger bandwidths, the same physical paths are resolved into a finer resolution.

phase causes selective fading in frequency. This says that $E_r(f, t)$ changes significantly, not only when t changes by $1/(4D_s)$, but also when f changes by $1/(2T_d)$. This argument extends to an arbitrary number of paths, so the *coherence bandwidth*, W_c, is given by

$$\boxed{W_c = \frac{1}{2T_d}.} \tag{2.47}$$

This relationship, like (2.44), is intended as an order of magnitude relation, essentially pointing out that the coherence bandwidth is reciprocal to the multipath spread. When the bandwidth of the input is considerably less than W_c, the channel is usually referred to as *flat fading*. In this case, the delay spread T_d is much less than the symbol time $1/W$, and a single channel filter tap is sufficient to represent the channel. When the bandwidth is much larger than W_c, the channel is said to be *frequency-selective*, and it has to be represented by multiple taps. Note that flat or frequency-selective fading is not a property of the channel alone, but of the relationship between the bandwidth W and the coherence bandwidth T_d (Figure 2.13).

The physical parameters and the time-scale of change of key parameters of the discrete-time baseband channel model are summarized in Table 2.1. The different types of channels are summarized in Table 2.2.

Table 2.1 A summary of the physical parameters of the channel and the time-scale of change of the key parameters in its discrete-time baseband model.

Key channel parameters and time-scales	Symbol	Representative values
Carrier frequency	f_c	1 GHz
Communication bandwidth	W	1 MHz
Distance between transmitter and receiver	d	1 km
Velocity of mobile	v	64 km/h
Doppler shift for a path	$D = f_c v/c$	50 Hz
Doppler spread of paths corresponding to a tap	D_s	100 Hz
Time-scale for change of path amplitude	d/v	1 minute
Time-scale for change of path phase	$1/(4D)$	5 ms
Time-scale for a path to move over a tap	$c/(vW)$	20 s
Coherence time	$T_c = 1/(4D_s)$	2.5 ms
Delay spread	T_d	1 μs
Coherence bandwidth	$W_c = 1/(2T_d)$	500 kHz

Table 2.2 A summary of the types of wireless channels and their defining characteristics.

Types of channel	Defining characteristic
Fast fading	$T_c \ll$ delay requirement
Slow fading	$T_c \gg$ delay requirement
Flat fading	$W \ll W_c$
Frequency-selective fading	$W \gg W_c$
Underspread	$T_d \ll T_c$

2.4 Statistical channel models

2.4.1 Modeling philosophy

We defined Doppler spread and multipath spread in the previous section as quantities associated with a given receiver at a given location, velocity, and time. However, we are interested in a characterization that is valid over some range of conditions. That is, we recognize that the channel filter taps $\{h_\ell[m]\}$ must be measured, but we want a statistical characterization of how many taps are necessary, how quickly they change and how much they vary.

Such a characterization requires a probabilistic model of the channel tap values, perhaps gathered by statistical measurements of the channel. We are familiar with describing additive noise by such a probabilistic model (as a Gaussian random variable). We are also familiar with evaluating error probability while communicating over a channel using such models. These

error probability evaluations, however, depend critically on the independence and Gaussian distribution of the noise variables.

It should be clear from the description of the physical mechanisms generating Doppler spread and multipath spread that probabilistic models for the channel filter taps are going to be far less believable than the models for additive noise. On the other hand, we need such models, even if they are quite inaccurate. Without models, systems are designed using experience and experimentation, and creativity becomes somewhat stifled. Even with highly over-simplified models, we can compare different system approaches and get a sense of what types of approaches are worth pursuing.

To a certain extent, all analytical work is done with simplified models. For example, white Gaussian noise (WGN) is often assumed in communication models, although we know the model is valid only over sufficiently small frequency bands. With WGN, however, we expect the model to be quite good when used properly. For wireless channel models, however, probabilistic models are quite poor and only provide order-of-magnitude guides to system design and performance. We will see that we can define Doppler spread, multipath spread, etc. much more cleanly with probabilistic models, but the underlying problem remains that these channels are very different from each other and cannot really be characterized by probabilistic models. At the same time, there is a large literature based on probabilistic models for wireless channels, and it has been highly useful for providing insight into wireless systems. However, it is important to understand the robustness of results based on these models.

There is another question in deciding what to model. Recall the continuous-time multipath fading channel

$$y(t) = \sum_i a_i(t)x(t - \tau_i(t)) + w(t). \tag{2.48}$$

This contains an exact specification of the delay and magnitude of each path. From this, we derived a discrete-time baseband model in terms of channel filter taps as

$$y[m] = \sum_\ell h_\ell[m]x[m - \ell] + w[m], \tag{2.49}$$

where

$$h_\ell[m] = \sum_i a_i(m/W)\mathrm{e}^{-\mathrm{j}2\pi f_c \tau_i(m/W)}\mathrm{sinc}[\ell - \tau_i(m/W)W]. \tag{2.50}$$

We used the sampling theorem expansion in which $x[m] = x_\mathrm{b}(m/W)$ and $y[m] = y_\mathrm{b}(m/W)$. Each channel tap $h_\ell[m]$ contains an aggregate of paths, with the delays smoothed out by the baseband signal bandwidth.

Fortunately, it is the filter taps that must be modeled for input/output descriptions, and also fortunately, the filter taps often contain a sufficient path aggregation so that a statistical model might have a chance of success.

2.4.2 Rayleigh and Rician fading

The simplest probabilistic model for the channel filter taps is based on the assumption that there are a large number of statistically independent reflected and scattered paths with random amplitudes in the delay window corresponding to a single tap. The phase of the ith path is $2\pi f_c \tau_i$ modulo 2π. Now, $f_c\tau_i = d_i/\lambda$, where d_i is the distance travelled by the ith path and λ is the carrier wavelength. Since the reflectors and scatterers are far away relative to the carrier wavelength, i.e., $d_i \gg \lambda$, it is reasonable to assume that the phase for each path is uniformly distributed between 0 and 2π and that the phases of different paths are independent. The contribution of each path in the tap gain $h_\ell[m]$ is

$$a_i(m/W)\mathrm{e}^{-\mathrm{j}2\pi f_c \tau_i(m/W)}\mathrm{sinc}[\ell - \tau_i(m/W)W] \tag{2.51}$$

and this can be modeled as a circular symmetric complex random variable.[8] Each tap $h_\ell[m]$ is the sum of a large number of such small independent circular symmetric random variables. It follows that $\Re(h_\ell[m])$ is the sum of many small independent real random variables, and so by the Central Limit Theorem, it can reasonably be modeled as a zero-mean Gaussian random variable. Similarly, because of the uniform phase, $\Re(h_\ell[m]\mathrm{e}^{\mathrm{j}\phi})$ is Gaussian with the same variance for any fixed ϕ. This assures us that $h_\ell[m]$ is in fact circular symmetric $\mathcal{CN}(0, \sigma_\ell^2)$ (see Section A.1.3 in Appendix A for an elaboration). It is assumed here that the variance of $h_\ell[m]$ is a function of the tap ℓ, but independent of time m (there is little point in creating a probabilistic model that depends on time). With this assumed Gaussian probability density, we know that the magnitude $|h_\ell[m]|$ of the ℓth tap is a *Rayleigh* random variable with density (cf. (A.20) in Appendix A and Exercise 2.14)

$$\boxed{\frac{x}{\sigma_\ell^2}\exp\left\{\frac{-x^2}{2\sigma_\ell^2}\right\}, \quad x \geq 0,} \tag{2.52}$$

and the squared magnitude $|h_\ell[m]|^2$ is exponentially distributed with density

$$\boxed{\frac{1}{\sigma_\ell^2}\exp\left\{\frac{-x}{\sigma_\ell^2}\right\}, \quad x \geq 0.} \tag{2.53}$$

This model, which is called *Rayleigh fading*, is quite reasonable for scattering mechanisms where there are many small reflectors, but is adopted primarily for its simplicity in typical cellular situations with a relatively small number of reflectors. The word *Rayleigh* is almost universally used for this

[8] See Section A.1.3 in Appendix A for a more in-depth discussion of circular symmetric random variables and vectors.

model, but the assumption is that the tap gains are circularly symmetric complex Gaussian random variables.

There is a frequently used alternative model in which the line-of-sight path (often called a *specular* path) is large and has a known magnitude, and that there are also a large number of independent paths. In this case, $h_\ell[m]$, at least for one value of ℓ, can be modeled as

$$\boxed{h_\ell[m] = \sqrt{\frac{\kappa}{\kappa+1}}\sigma_\ell e^{j\theta} + \sqrt{\frac{1}{\kappa+1}}\mathcal{CN}\left(0, \sigma_\ell^2\right)} \tag{2.54}$$

with the first term corresponding to the specular path arriving with uniform phase θ and the second term corresponding to the aggregation of the large number of reflected and scattered paths, independent of θ. The parameter κ (so-called K-factor) is the ratio of the energy in the specular path to the energy in the scattered paths; the larger κ is, the more deterministic is the channel. The magnitude of such a random variable is said to have a *Rician* distribution. Its density has quite a complicated form; it is often a better model of fading than the Rayleigh model.

2.4.3 Tap gain auto-correlation function

Modeling each $h_\ell[m]$ as a complex random variable provides part of the statistical description that we need, but this is not the most important part. The more important issue is how these quantities vary with time. As we will see in the rest of the book, the rate of channel variation has significant impact on several aspects of the communication problem. A statistical quantity that models this relationship is known as the *tap gain auto-correlation function*, $R_\ell[n]$. It is defined as

$$R_\ell[n] := \mathbb{E}\left\{h_\ell^*[m]h_\ell[m+n]\right\}. \tag{2.55}$$

For each tap ℓ, this gives the auto-correlation function of the sequence of random variables modeling that tap as it evolves in time. We are tacitly assuming that this is not a function of time m. Since the sequence of random variables $\{h_\ell[m]\}$ for any given ℓ has both a mean and covariance function that does not depend on m, this sequence is wide-sense stationary. We also assume that, as a random variable, $h_\ell[m]$ is independent of $h_{\ell'}[m']$ for all $\ell \neq \ell'$ and all m, m'. This final assumption is intuitively plausible since paths in different ranges of delay contribute to $h_\ell[m]$ for different values of ℓ.[9]

The coefficient $R_\ell[0]$ is proportional to the energy received in the ℓth tap. The multipath spread T_d can be defined as the product of $1/W$ times the range of ℓ which contains most of the total energy $\sum_{\ell=0}^{\infty} R_\ell[0]$. This is

[9] One could argue that a moving reflector would gradually travel from the range of one tap to another, but as we have seen, this typically happens over a very large time-scale.

somewhat preferable to our previous "definition" in that the statistical nature of T_d becomes explicit and the reliance on some sort of stationarity becomes explicit. Now, we can also define the coherence time T_c more explicitly as the smallest value of $n > 0$ for which $R_\ell[n]$ is significantly different from $R_\ell[0]$. With both of these definitions, we still have the ambiguity of what "significant" means, but we are now facing the reality that these quantities must be viewed as statistics rather than as instantaneous values.

The tap gain auto-correlation function is useful as a way of expressing the statistics for how tap gains change given a particular bandwidth W, but gives little insight into questions related to choice of a bandwidth for communication. If we visualize increasing the bandwidth, we can see several things happening. First, the ranges of delay that are separated into different taps ℓ become narrower ($1/W$ seconds), so there are fewer paths corresponding to each tap, and thus the Rayleigh approximation becomes poorer. Second, the sinc functions of (2.50) become narrower, and $R_\ell[0]$ gives a finer grained picture of the amount of power being received in the ℓth delay window of width $1/W$. In summary, as we try to apply this model to larger W, we get more detailed information about delay and correlation at that delay, but the information becomes more questionable.

Example 2.2 Clarke's model

This is a popular statistical model for flat fading. The transmitter is fixed, the mobile receiver is moving at speed v, and the transmitted signal is scattered by stationary objects around the mobile. There are K paths, the ith path arriving at an angle $\theta_i := 2\pi i/K$, $i = 0, \ldots, K-1$, with respect to the direction of motion. K is assumed to be large. The scattered path arriving at the mobile at the angle θ has a delay of $\tau_\theta(t)$ and a time-invariant gain a_θ, and the input/output relationship is given by

$$y(t) = \sum_{i=0}^{K-1} a_{\theta_i} x(t - \tau_{\theta_i}(t)) \tag{2.56}$$

The most general version of the model allows the received power distribution $p(\theta)$ and the antenna gain pattern $\alpha(\theta)$ to be arbitrary functions of the angle θ, but the most common scenario assumes uniform power distribution and isotropic antenna gain pattern, i.e., the amplitudes $a_\theta = a/\sqrt{K}$ for all angles θ. This models the situation when the scatterers are located in a ring around the mobile (Figure 2.14). We scale the amplitude of each path by $\sqrt{K}$ so that the total received energy along all paths is a^2; for large K, the received energy along each path is a small fraction of the total energy.

Suppose the communication bandwidth W is much smaller than the reciprocal of the delay spread. The complex baseband channel can be represented by a single tap at each time:

$$y[m] = h_0[m]x[m] + w[m]. \tag{2.57}$$

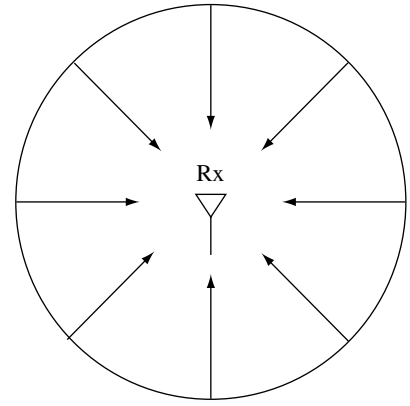

Figure 2.14 The one-ring model.

The phase of the signal arriving at time 0 from an angle θ is $2\pi f_c \tau_\theta(0)$ mod 2π, where f_c is the carrier frequency. Making the assumption that this phase is uniformly distributed in $[0, 2\pi]$ and independently distributed across all angles θ, the tap gain process $\{h_0[m]\}$ is a sum of many small independent contributions, one from each angle. By the Central Limit Theorem, it is reasonable to model the process as Gaussian. Exercise 2.17 shows further that the process is in fact stationary with an autocorrelation function $R_0[n]$ given by:

$$R_0[n] = 2a^2 \pi J_0 (n\pi D_s / W) \tag{2.58}$$

where $J_0(\cdot)$ is the zeroth-order Bessel function of the first kind:

$$J_0(x) := \frac{1}{\pi} \int_0^\pi e^{jx\cos\theta} d\theta. \tag{2.59}$$

and $D_s = 2f_c v/c$ is the Doppler spread. The power spectral density $S(f)$, defined on $[-1/2, +1/2]$, is given by

$$S(f) = \begin{cases} \frac{4a^2 W}{D_s \sqrt{1-(2fW/D_s)^2}} & -D_s/(2W) \leqslant f \leqslant +D_s/(2W) \\ 0 & \text{else.} \end{cases} \tag{2.60}$$

This can be verified by computing the inverse Fourier transform of (2.60) to be (2.58). Plots of the autocorrelation function and the spectrum for are shown in Figure 2.15. If we define the coherence time T_c to be the value of n/W such that $R_0[n] = 0.05 R_0[0]$, then

$$T_c = \frac{J_0^{-1}(0.05)}{\pi D_s}, \tag{2.61}$$

i.e., the coherence time is inversely proportional to D_s.

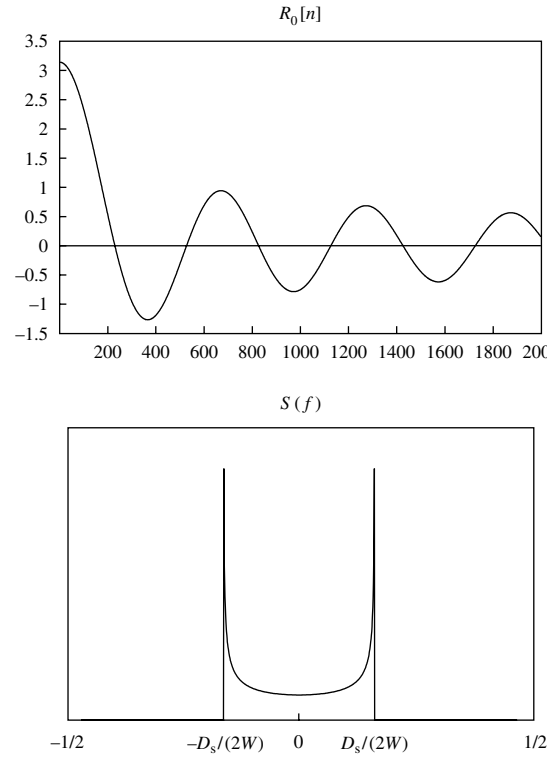

Figure 2.15 Plots of the auto-correlation function and Doppler spectrum in Clarke's model.

In Exercise 2.17, you will also verify that $S(f)\mathrm{d}f$ has the physical interpretation of the received power along paths that have Doppler shifts in the range $[f, f+\mathrm{d}f]$. Thus, $S(f)$ is also called the *Doppler spectrum*. Note that $S(f)$ is zero beyond the maximum Doppler shift.

Chapter 2 The main plot

Large-scale fading
Variation of signal strength over distances of the order of cell sizes. Received power decreases with distance r like:

$$\frac{1}{r^2} \quad \text{(free space)}$$

$$\frac{1}{r^4} \quad \text{(reflection from ground plane).}$$

Decay can be even faster due to shadowing and scattering effects.

Small-scale fading

Variation of signal strength over distances of the order of the carrier wavelength, due to constructive and destructive interference of multipaths. Key parameters:

$$\text{Doppler spread } D_{\text{s}} \longleftrightarrow \text{coherence time } T_{\text{c}} \sim 1/D_{\text{s}}$$

Doppler spread is proportional to the velocity of the mobile and to the angular spread of the arriving paths.

$$\text{delay spread } T_{\text{d}} \longleftrightarrow \text{coherence bandwidth } W_{\text{c}} \sim 1/T_{\text{d}}$$

Delay spread is proportional to the difference between the lengths of the shortest and the longest paths.

Input/output channel models

- Continuous-time passband (2.14):

$$y(t) = \sum_i a_i(t) x(t - \tau_i(t)).$$

- Continuous-time complex baseband (2.26):

$$y_{\text{b}}(t) = \sum_i a_i(t) \mathrm{e}^{-\mathrm{j}2\pi f_{\text{c}} \tau_i(t)} x_{\text{b}}(t - \tau_i(t)).$$

- Discrete-time complex baseband with AWGN (2.38):

$$y[m] = \sum_\ell h_\ell[m] x[m - \ell] + w[m].$$

The ℓth tap is the aggregation of the physical paths with delays in $[\ell/W - 1/(2W), \ell/W + 1/(2W)]$.

Statistical channel models

- $\{h_\ell[m]\}_m$ is modeled as circular symmetric processes independent across the taps.
- If for all taps,

$$h_\ell[m] \sim \mathcal{CN}(0, \sigma_\ell^2),$$

  the model is called *Rayleigh*.
- If for one tap,

$$h_\ell[m] = \sqrt{\frac{\kappa}{\kappa+1}} \sigma_\ell \mathrm{e}^{\mathrm{j}\theta} + \sqrt{\frac{1}{\kappa+1}} \mathcal{CN}(0, \sigma_\ell^2),$$

  the model is called *Rician* with K-factor κ.

- The tap gain auto-correlation function $R_\ell[n] := \mathbb{E}[h_\ell^*[0]h_\ell[n]]$ models the dependency over time.
- The delay spread is $1/W$ times the range of taps ℓ which contains most of the total gain $\sum_{\ell=0}^{\infty} R_\ell[0]$. The coherence time is $1/W$ times the range of n for which $R_\ell[n]$ is significantly different from $R_\ell[0]$.

2.5 Bibliographical notes

This chapter was modified from R. G. Gallager's MIT 6.450 course notes on digital communication. The focus is on small-scale multipath fading. Large-scale fading models are discussed in many texts; see for example Rappaport [98]. Clarke's model was introduced in [22] and elaborated further in [62]. Our derivation here of the Clarke power spectrum follows the approach of [111].

2.6 Exercises

Exercise 2.1 (Gallager) Consider the electric field in (2.4).

1. It has been derived under the assumption that the motion is in the direction of the line-of-sight from sending antenna to receive antenna. Find the electric field assuming that ϕ is the angle between the line-of-sight and the direction of motion of the receiver. Assume that the range of time of interest is small enough so that changes in (θ, ψ) can be ignored.
2. Explain why, and under what conditions, it is a reasonable approximation to ignore the change in (θ, ψ) over small intervals of time.

Exercise 2.2 (Gallager) Equation (2.13) was derived under the assumption that $r(t) \approx d$. Derive an expression for the received waveform for general $r(t)$. Break the first term in (2.11) into two terms, one with the same numerator but the denominator $2d - r_0 - vt$ and the other with the remainder. Interpret your result.

Exercise 2.3 In the two-path example in Sections 2.1.3 and 2.1.4, the wall is on the right side of the receiver so that the reflected wave and the direct wave travel in opposite directions. Suppose now that the reflecting wall is on the left side of transmitter. Redo the analysis. What is the nature of the multipath fading, both over time and over frequency? Explain any similarity or difference with the case considered in Sections 2.1.3 and 2.1.4.

Exercise 2.4 A mobile receiver is moving at a speed v and is receiving signals arriving along two reflected paths which make angles θ_1 and θ_2 with the direction of motion. The transmitted signal is a sinusoid at frequency f.

1. Is the above information enough for estimating (i) the coherence time T_c; (ii) the coherence bandwidth W_c? If so, express them in terms of the given parameters. If not, specify what additional information would be needed.
2. Consider an environment in which there are reflectors and scatterers in all directions from the receiver and an environment in which they are clustered within a small

angular range. Using part (1), explain how the channel would differ in these two environments.

Exercise 2.5 Consider the propagation model in Section 2.1.5 where there is a reflected path from the ground plane.

1. Let r_1 be the length of the direct path in Figure 2.6. Let r_2 be the length of the reflected path (summing the path length from the transmitter to the ground plane and the path length from the ground plane to the receiver). Show that $r_2 - r_1$ is asymptotically equal to b/r and find the value of the constant b. *Hint*: Recall that for x small, $\sqrt{1+x} \approx 1 + x/2$ in the sense that $(\sqrt{1+x} - 1)/x \to 1/2$ as $x \to 0$.
2. Assume that the received waveform at the receive antenna is given by

$$E_{\mathrm{r}}(f, t) = \frac{\alpha \cos 2\pi[ft - fr_1/c]}{r_1} - \frac{\alpha \cos 2\pi[ft - fr_2/c]}{r_2}. \tag{2.62}$$

   Approximate the denominator r_2 by r_1 in (2.62) and show that $E_{\mathrm{r}} \approx \beta/r^2$ for r^{-1} much smaller than c/f. Find the value of β.
3. Explain why this asymptotic expression remains valid without first approximating the denominator r_2 in (2.62) by r_1.

Exercise 2.6 Consider the following simple physical model in just a *single* dimension. The source is at the origin and transmits an isotropic wave of angular frequency ω. The physical environment is filled with uniformly randomly located obstacles. We will model the inter-obstacle distance as an exponential random variable, i.e., it has the density[10]

$$\eta \mathrm{e}^{-\eta r}, \qquad r \geq 0. \tag{2.63}$$

Here $1/\eta$ is the mean distance between obstacles and captures the *density* of the obstacles. Viewing the source as a stream of photons, suppose each obstacle independently (from one photon to the other and independent of the behavior of the other obstacles) either absorbs the photon with probability γ or scatters it either to the left or to the right (both with equal probability $(1-\gamma)/2$).

Now consider the path of a photon transmitted either to the left or to the right with equal probability from some fixed point on the line. The probability density function of the distance (denoted by r) to the first obstacle (the distance can be on either side of the starting point, so r takes values on the entire line) is equal to

$$q(r) := \frac{\eta \mathrm{e}^{-\eta|r|}}{2}, \qquad r \in \mathcal{R}. \tag{2.64}$$

So the probability density function of the distance at which the photon is absorbed upon hitting the first obstacle is equal to

$$f_1(r) := \gamma q(r), \qquad r \in \mathcal{R}. \tag{2.65}$$

[10] This random arrangement of points on a line is called a *Poisson point process*.

1. Show that the probability density function of the distance from the origin at which the second obstacle is met is

$$f_2(r) := \int_{-\infty}^{\infty} (1-\gamma) q(x) f_1(r-x) \mathrm{d}x, \qquad r \in \mathcal{R}. \tag{2.66}$$

2. Denote by $f_k(r)$ the probability density function of the distance from the origin at which the photon is absorbed by exactly the kth obstacle it hits and show the recursive relation

$$f_{k+1}(r) = \int_{-\infty}^{\infty} (1-\gamma) q(x) f_k(r-x) \mathrm{d}x, \qquad r \in \mathcal{R}. \tag{2.67}$$

3. Conclude from the previous step that the probability density function of the distance from the source at which the photon is absorbed (by some obstacle), denoted by $f(r)$, satisfies the recursive relation

$$f(r) = \gamma q(r) + (1-\gamma) \int_{-\infty}^{\infty} q(x) f(r-x) \mathrm{d}x, \qquad r \in \mathcal{R}. \tag{2.68}$$

   Hint: Observe that $f(r) = \sum_{k=1}^{\infty} f_k(r)$.
4. Show that

$$f(r) = \frac{\sqrt{\gamma}\eta}{2} \mathrm{e}^{-\eta\sqrt{\gamma}|r|} \tag{2.69}$$

   is a solution to the recursive relation in (2.68). *Hint*: Observe that the convolution between the probability densities $q(\cdot)$ and $f(\cdot)$ in (2.68) is more easily represented using Fourier transforms.
5. Now consider the photons that are absorbed at a distance of more than r from the source. This is the radiated power density at a distance r and is found by integrating $f(x)$ over the range (r, ∞) if $r > 0$ and $(-\infty, r)$ if $r < 0$. Calculate the radiated power density to be

$$\frac{\mathrm{e}^{-\gamma\sqrt{\eta}|r|}}{2}, \tag{2.70}$$

   and conclude that the power decreases exponentially with distance r. Also observe that with very low absorption ($\gamma \to 0$) or very few obstacles ($\eta \to 0$), the power density converges to 0.5; this is expected since the power splits equally on either side of the line.

Exercise 2.7 In Exercise 2.6, we considered a single-dimensional physical model of a scattering and absorption environment and concluded that power decays exponentially with distance. A reading exercise is to study [42], which considers a natural extension of this simple model to two- and three-dimensional spaces. Further, it extends the analysis to two- and three-dimensional physical models. While the analysis is more complicated, we arrive at the same conclusion: the radiated power decays exponentially with distance.

Exercise 2.8 (Gallager) Assume that a communication channel first filters the transmitted passband signal before adding WGN. Suppose the channel is known and the channel filter has an impulse response $h(t)$. Suppose that a QAM scheme with symbol duration T is developed without knowledge of the channel filtering. A baseband filter $\theta(t)$ is developed satisfying the Nyquist property that $\{\theta(t-kT)\}_k$ is an orthonormal set. The matched filter $\theta(-t)$ is used at the receiver before sampling and detection.

If one is aware of the channel filter $h(t)$, one may want to redesign either the baseband filter at the transmitter or the baseband filter at the receiver so that there is no intersymbol interference between receiver samples and so that the noise on the samples is i.i.d.

1. Which filter should one redesign?
2. Give an expression for the impulse response of the redesigned filter (assume a carrier frequency f_c).
3. Draw a figure of the various filters at passband to show why your solution is correct. (We suggest you do this before answering the first two parts.)

Exercise 2.9 Consider the two-path example in Section 2.1.4 with $d = 2\,\text{km}$ and the receiver at 1.5 km from the transmitter moving at velocity 60 km/h away from the transmitter. The carrier frequency is 900 MHz.

1. Plot in MATLAB the magnitudes of the taps of the discrete-time baseband channel at a fixed time t. Give a few plots for several bandwidths W so as to exhibit both flat and frequency-selective fading.
2. Plot the time variation of the phase and magnitude of a typical tap of the discrete-time baseband channel for a bandwidth where the channel is (approximately) flat and for a bandwidth where the channel is frequency-selective. How do the time-variations depend on the bandwidth? Explain.

Exercise 2.10 For each tap of the discrete-time channel response, the Doppler spread is the range of Doppler shifts of the paths contributing to that tap. Give an example of an environment (i.e. location of reflectors/scatterers with respect to the location of the transmitter and the receiver) in which the Doppler spread is the same for different taps and an environment in which they are different.

Exercise 2.11 Verify (2.39) and (2.40).

Exercise 2.12 In this problem we consider generating passband orthogonal waveforms from baseband ones.

1. Show that if the waveforms $\{\theta(t-nT)\}_n$ form an orthogonal set, then the waveforms $\{\psi_{n,1}, \psi_{n,2}\}_n$ also form an orthogonal set, provided that $\theta(t)$ is band-limited to $[-f_c, f_c]$. Here,

$$\psi_{n,1}(t) = \theta(t-nT)\cos 2\pi f_c t,$$
$$\psi_{n,2}(t) = \theta(t-nT)\sin 2\pi f_c t.$$

   How should we normalize the energy of $\theta(t)$ to make the $\psi(t)$ *orthonormal*?
2. For a given f_c, find an example where the result in part (1) is false when the condition that $\theta(t)$ is band-limited to $[-f_c, f_c]$ is violated.

Exercise 2.13 Verify (2.25). Does this equation contain any more information about the communication system in Figure 2.9 beyond what is in (2.24)? Explain.

Exercise 2.14 Compute the probability density function of the magnitude $|X|$ of a complex circular symmetric Gaussian random variable X with variance σ^2.

Exercise 2.15 In the text we have discussed the various reasons why the channel tap gains, $h_\ell[m]$, vary in time (as a function of m) and how the various dynamics operate at different time-scales. The analysis is based on the assumption that communication takes place on a bandwidth W around a carrier frequency f_c with $f_c \gg W$. This assumption is not valid for *ultra-wideband* (UWB) communication systems, where the transmission bandwidth is from 3.1 GHz to 10.6 GHz, as regulated by the FCC. Redo the analysis for this system. What is the main mechanism that causes the tap gains to vary at the fastest time-scale, and what is this fastest time-scale determined by?

Exercise 2.16 In Section 2.4.2, we argue that the channel gain $h_\ell[m]$ at a particular time m can be assumed to be circular symmetric. Extend the argument to show that it is also reasonable to assume that the complex random vector

$$\mathbf{h} := \begin{pmatrix} h_\ell[m] \\ h_\ell[m+1] \\ \vdots \\ h_\ell[m+n] \end{pmatrix}$$

is circular symmetric for any n.

Exercise 2.17 In this question, we will analyze in detail Clarke's one-ring model discussed at the end of the chapter. Recall that the scatterers are assumed to be located in a ring around the receiver moving at speed v. There are K paths coming in at angles $\theta_i = 2\pi i/K$ with respect to the direction of motion of the mobile, $i = 0, \ldots, K-1$. The path coming at angle θ has a delay of $\tau_\theta(t)$ and a time-invariant gain $a/\sqrt{K}$ (not dependent on the angle), and the input/output relationship is given by

$$y(t) = \frac{a}{\sqrt{K}} \sum_{i=0}^{K-1} x(t - \tau_{\theta_i}(t)). \tag{2.71}$$

1. Give an expression for the impulse response $h(\tau, t)$ for this channel, and give an expression for $\tau_\theta(t)$ in terms of $\tau_\theta(0)$. (You can assume that the distance the mobile travelled in $[0, t]$ is small compared to the radius of the ring.)
2. Suppose communication takes place at carrier frequency f_c and over a narrowband of bandwidth W such that the delay spread of the channel T_d satisfies $T_d \ll 1/W$. Argue that the discrete-time baseband model can be approximately represented by a single tap

   $$y[m] = h_0[m]x[m] + w[m], \tag{2.72}$$

   and give an approximate expression for that tap in terms of the a_θ's and $\tau_\theta(t)$'s. *Hint*: Your answer should contain no sinc functions.
3. Argue that it is reasonable to assume that the phase of the path from an angle θ at time 0,

   $$2\pi f_c \tau_\theta(0) \mod 2\pi$$

   is uniformly distributed in $[0, 2\pi]$ and that it is i.i.d. across θ.

4. Based on the assumptions in part (3), for large K one can use the Central Limit Theorem to approximate $\{h_0[m]\}$ as a Gaussian process. Verify that the limiting process is stationary and the autocorrelation function $R_0[n]$ is given by (2.58).
5. Verify that the Doppler spectrum $S(f)$ is given by (2.60). *Hint*: It is easier to show that the inverse Fourier transform of (2.60) is (2.58).
6. Verify that $S(f)\mathrm{d}f$ is indeed the received power from the paths that have Doppler shifts in $[f, f+\mathrm{d}f]$. Is this surprising?

Exercise 2.18 Consider a one-ring model where there are K scatterers located at angles $\theta_i = 2\pi i/K$, $i = 0, \ldots, K-1$, on a circle of radius 1 km around the receiver and the transmitter is 2 km away. (The angles are with respect to the line joining the transmitter and the receiver.) The transmit power is P. The power attenuation along a path from the transmitter to a scatterer to the receiver is

$$\frac{G}{K} \cdot \frac{1}{s^2} \cdot \frac{1}{r^2}, \tag{2.73}$$

where G is a constant and r and s are the distance from the transmitter to the scatterer and the distance from the scatterer to the receiver respectively. Communication takes place at a carrier frequency $f_c = 1.9$ GHz and the bandwidth is W Hz. You can assume that, at any time, the phases of each arriving path in the baseband representation of the channel are independent and uniformly distributed between 0 and 2π.

1. What are the key differences and the similarities between this model and the Clarke's model in the text?
2. Find approximate conditions on the bandwidth W for which one gets a flat fading channel.
3. Suppose the bandwidth is such that the channel is frequency selective. For large K, find approximately the amount of power in tap ℓ of the discrete-time baseband impulse response of the channel (i.e., compute the power-delay profile.). Make any simplifying assumptions but state them. (You can leave your answers in terms of integrals if you cannot evaluate them.)
4. Compute and sketch the power-delay profile as the bandwidth becomes very large (and K is large).
5. Suppose now the receiver is moving at speed v towards the (fixed) transmitter. What is the Doppler spread of tap ℓ? Argue heuristically from physical considerations what the Doppler spectrum (i.e., power spectral density) of tap ℓ is, for large K.
6. We have made the assumptions that the scatterers are all on a circle of radius 1km around the receiver and the paths arrive with independent and uniform distributed phases at the receiver. Mathematically, are the two assumptions consistent? If not, do you think it matters, in terms of the validity of your answers to the earlier parts of this question?

Exercise 2.19 Often in modeling multiple input multiple output (MIMO) fading channels the fading coefficients between different transmit and receive antennas are assumed to be independent random variables. This problem explores whether this is a reasonable assumption based on Clarke's one-ring scattering model and the antenna separation.

1. (Antenna separation at the mobile) Assume a mobile with velocity v moving away from the base-station, with uniform scattering from the ring around it.

(a) Compute the Doppler spread D_s for a carrier frequency f_c, and the corresponding coherence time T_c.

(b) Assuming that fading states separated by T_c are approximately uncorrelated, at what distance should we place a second antenna at the mobile to get an independently faded signal? *Hint*: How much distance does the mobile travel in T_c?

2. (Antenna separation at the base-station) Assume that the scattering ring has radius R and that the distance between the base-station and the mobile is d. Further assume for the time being that the base-station is moving away from the mobile with velocity v'. Repeat the previous part to find the minimum antenna spacing at the base-station for uncorrelated fading. *Hint*: Is the scattering still uniform around the base-station?
3. Typically, the scatterers are local around the mobile (near the ground) and far away from the base-station (high on a tower). What is the implication of your result in part (2) for this scenario?